FeIII and FeII Phosphasalen Complexes: Synthesis, Characterization, and Catalytic Application for 2-Naphtol Oxidative Coupling

Emmanuel Oheix, Christian Herrero, Jules Moutet, Jean-noël Rebilly, Marie Cordier, Régis Guillot,, Sophie Bourcier, Fréderic Banse, Katell Sénéchal-David, Audrey Auffrant

▶ **To cite this version:**

Emmanuel Oheix, Christian Herrero, Jules Moutet, Jean-noël Rebilly, Marie Cordier, et al.. FeIII and FeII Phosphasalen Complexes: Synthesis, Characterization, and Catalytic Application for 2-Naphtol Oxidative Coupling. Chemistry - A European Journal, 2020, 10.1002/chem.202001662 . hal-02938996

HAL Id: hal-02938996
https://hal.science/hal-02938996

Submitted on 15 Sep 2020

HAL is a multi-disciplinary open access archive for the deposit and dissemination of scientific research documents, whether they are published or not. The documents may come from teaching and research institutions in France or abroad, or from public or private research centers.

L'archive ouverte pluridisciplinaire **HAL**, est destinée au dépôt et à la diffusion de documents scientifiques de niveau recherche, publiés ou non, émanant des établissements d'enseignement et de recherche français ou étrangers, des laboratoires publics ou privés.

Fe^{III} and Fe^{II} phosphasalen complexes: Synthesis, characterization, and catalytic application for 2-naphtol oxidative coupling

Emmanuel Oheix,[a,b] Christian Herrero,[b] Jules Moutet,[a] Jean-Noël Rebilly,[b] Marie Cordier,[a] Régis Guillot,[b] Sophie Bourcier,[a] Frédéric Banse,[b]* Katell Sénéchal-David,[b]* Audrey Auffrant. [a]*

[a] Dr. E. Oheix, Dr. J. Moutet, Ms M. Cordier, Dr. S. Bourcier, Dr. A. Auffrant)
Laboratoire de Chimie Moléculaire,
CNRS UMR 9168, École Polytechnique, Institut Polytechnique de Paris , 91128 Palaiseau, France
E-mail: Audrey.auffrant@polytechnique.edu

[b] Dr. E. Oheix, Dr. C. Herrero, Dr. J.-N. Rebilly, Dr Régis Guillot, Pr. F. Banse, Dr. K. Sénéchal-David
Université Paris-Saclay, CNRS, Institut de Chimie Moléculaire et des Matériaux d'Orsay, 91405, Orsay, France.
E-mail: frederic.banse@universite-paris-saclay.fr, katell.senechal-david@universite-paris-saclay.fr

Supporting information for this article is given via a link at the end of the document.

Abstract: Synthesis and characterization of three iron(III) phosphasalen complexes as well as the iron(II) analogue are reported. Phosphasalen (Psalen) differ from salen by the presence of iminophosphorane (P=N) functions in place of the imines in salen. All the complexes were characterized by single-crystal X-ray diffraction, UV-vis and EPR spectroscopy as well as cyclic voltammetry. The [Fe^{II}(Psalen)] complex was shown to remain tetracoordinated even in coordinating solvent but exhibits surprisingly a magnetic moment in line with a Fe^{II} high spin ground state. For the Fe^{III} complexes, the higher lability of triflate anion compared to nitrate was demonstrated. As they exhibit lower reduction potential compared to their salen analogues, these complexes were tested for the coupling of 2-naphtol using O_2 from air as oxidant. In order to shed light on this reaction, the interaction between 2-napthol and the Fe^{III}(Psalen) complexes was studied by cyclic voltammetry as well as UV-vis spectrosocopy.

Introduction

The presence of iron at the active site of many enzymatic systems has stimulated the synthesis of a variety of non-heme iron complexes in which the iron cation is generally stabilized by oxygen and/or nitrogen based ligands.[1] Salen-type ligands associating two nitrogen donors (imine or amine) and two phenolates are very popular to develop enzymatic mimics because of their easy synthesis and their high modularity. Despite the numerous structural variations performed on the salen ligand skeleton, few have consisted in introducing heteroatoms as we did some years ago when developing the phosphasalen (Psalen) platform,[2] in which imines are replaced by iminophosphoranes (P=N). This ligand is more electron-donating than salen because of the strong σ and π donor ability of the iminophosphorane. It was shown to be able to stabilize high valent copper and nickel complexes.[3] We therefore get interested in studying iron(III) and iron(II) Psalen complexes and their catalytic activity in oxidative coupling.

Oxidative coupling constitutes a viable method for the formation of C-C bond from unactivated C-H bonds.[4] In Nature, many such couplings are catalyzed by copper-containing oxidase enzymes and involve dioxygen as oxidant.[5] In the laboratory, the scope of these reactions is limited by selectivity issues, resulting from radical delocalization within the intermediates.[6] As an example, the homocoupling of phenol can lead to no less than 7 different products including 3 different regio-isomers of bisphenol.[7] In contrast, the coupling of 2-naphthol is highly selective in favor of the 1,1'-product. Moreover the oxidation potential of 2-naphthol being lower than that of phenol,[8] its oxidation is easier. Hence, 2-naphthol coupling is a widely applicable test reaction to study the electronic factors governing the oxidative coupling processes. However, reports of iron-catalyzed 2-naphthol coupling using dioxygen as the sole oxidant are scarce. Katsuki and co-workers reported the diastereoselective coupling of 2-naphthol under aerobic conditions using a chiral [Fe^{III}(Salan)] catalyst.[9] The conventional mechanism for Fe-catalyzed coupling of phenol derivatives involves an electron-transfer from Fe^{III}-phenoxo to form a Fe^{II}-phenoxyl radical cation species.[6a] In contrast, the kinetic studies performed by Katsuki and co-workers support a different mechanism, which involves one electron oxidation of the Fe^{III}-naphthoxo species to Fe^{IV}-naphthoxo (or Fe^{III}-naphthoxyl radical cation) as the rate-determining step.[10]

We anticipated that Psalen iron complexes with electron-enriched iron centres should catalyze this reaction. For this initial study, we selected from our library, a ligand bearing an achiral ethylene linker between the nitrogen atoms and *tert*-butyl groups on the *ortho*- and *para*- positions of the phenoxides to prevent side-reactions at these positions (Scheme 1). Besides, the nature of the exogenous ligand was previously shown to significantly modulate the redox potential in a series of iron complexes.[11] For this reason, we report on the synthesis of three **[Fe^{III}(Psalen)(X)]** complexes differing in the nature of the exogenous ligand/counter-anion X (Cl, NO_3, OTf) provided by the Fe^{III} reactant, and the neutral **[Fe^{II}(Psalen)]** complex. These complexes were studied in the solid-state (X-ray diffraction, EPR) and in solution (cyclic voltammetry, UV-visible and EPR). Interestingly, the Fe^{II} complex remains firmly tetravalent and no anion or solvent coordination was observed. Regarding the Fe^{III} complexes, our results clearly demonstrate that an acetonitrile or water molecule from the solvent can quantitatively displace the labile triflate exogenous ligand but not the chloride or nitrate. The influence of the counter-anion and solvent coordination on 2-naphthol coupling catalysis is also reported.

Results and Discussion

Synthesis and solid-state structures

The phosphasalen ligand **Psalen** was synthesized from the corresponding bis(aminophosphonium) salt as previously described.[12] It was then reacted with the appropriate iron precursor in THF. After removing the potassium salts by centrifugation, the residue obtained was washed with pentane, the complexes **[Fe^{III}(Psalen)Cl]**, **[Fe^{III}(Psalen)(NO$_3$)]** and **[Fe^{III}(Psalen)(OTf)]** were isolated in respectively 54, 64, and 80 % yield. The iron(II) complex was prepared in the glovebox by two different manners which gave similar results: the reaction of **Psalen** with [$FeCl_2(THF)_{1.5}$] in THF or the reaction with [$Fe(OTf)_2(CH_3CN)_2$] in acetonitrile. The diamagnetic zinc complex **[Zn(Psalen)]** was also synthesized from $ZnBr_2$ for comparison purpose.

The complexes were characterized by UV-vis spectroscopy, ESI-MS, and elemental analysis. Additionally, the diamagnetic complex **[Zn(Psalen)]** was characterized by ^{1}H, ^{13}C and ^{31}P NMR, whereas all paramagnetic Fe^{III} complexes were characterized by EPR instead (*vide infra*).

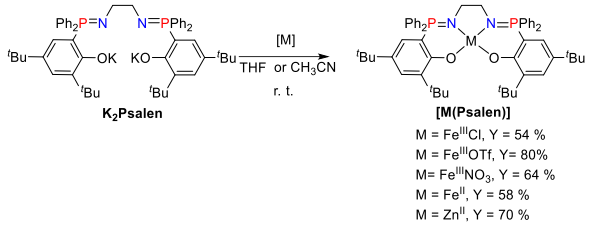

Scheme 1. Synthesis of Phosphasalen (Psalen) complexes

The structures of the Psalen iron complexes were studied by X-ray diffraction. Single crystals of **[Fe^{III}(Psalen)Cl]** were obtained from a saturated dichloromethane solution. The structure (Figure 1) shows the coordination of the phosphasalen N_2O_2 donor set and one chloro ligand. The observed geometry around iron is between a square-based pyramid and a trigonal bipyramid. Indeed, from the coordination angles, a τ_5[13] value of 0.238 was calculated indicating a slight preference for square-based pyramid geometry corresponding to $\tau_5 = 0$. Interestingly the τ_5 of the salen analogue[14] can be calculated at 0.475, a significantly higher value.

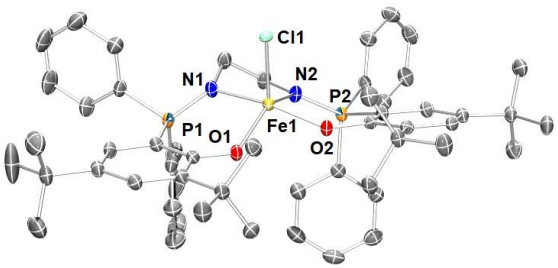

Figure 1. Ortep plot of **[Fe^{III}(Psalen)Cl]** crystallized from CH_2Cl_2 hydrogen atoms and solvent molecules were omitted for clarity.

The comparison of the coordination bonds shows that while the Fe-N are slightly shortened in the Psalen complex compared to the salen ones, the Fe-O are on the contrary elongated (Table S3). Surprisingly, lengthening of both M-O and M-N bonds generally observed when going from salen to phosphasalen is not seen with this iron complex.[2, 3b, 15]

The structure obtained for **[Fe^{III}(Psalen)(NO$_3$)]** allows to observe an original κ^2-coordination of the nitrate anion resulting in a highly distorted octahedral geometry around the iron center (Figure 2). The two oxygen of the nitrate are forced into *cis*-positions and thus impose a tight coordination angle (57.79(9)°). The two remaining in-plane positions are occupied by N2 and O1 with a broad angle O1-Fe-N2 (125.96(10)°). Finally, the axial positions of the octahedron are occupied by N1 and O2 (O2-Fe-N1 = 168.80(10)°). Compared to the structure of **[Fe^{III}(Psalen)Cl]**, the bonds and angles around the iron are of similar magnitude. Moreover, the structure of **[Fe^{III}(Psalen)(NO$_3$)]** resembles that published for a salen analogue,[16] and as for the chloride derivatives, changing from salen to Psalen induces an elongation of the Fe-O and a slight shortening of the Fe-N (Table S4).

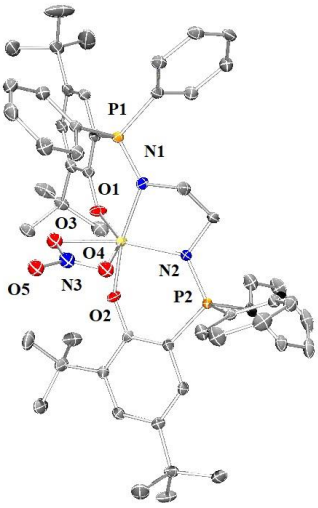

Figure 2. Ortep plot of **[Fe^{III}(Psalen)(NO$_3$)]**: hydrogen atoms were omitted for clarity

When crystallized from a saturated cyclohexane solution in the glovebox, the **[Fe^{III}(Psalen)(OTf)]** complex shows a pentacoordinate Fe^{III} coordinated to the phosphasalen N_2O_2 donor set and one oxygen from the triflate exogenous ligand (Figure 3, top). The geometry is a distorted square based pyramid with a τ_5 of 0.43.

The Fe-N and Fe-O bonds are slightly shorter compared to those measured in the chloride complex, which may be explained by a better donating ability of chloride compared to triflate. No comparable structure was found in the salen series precluding comparison.

Interestingly, when the crystallization of **[Fe^{III}(Psalen)(OTf)]** is performed without a protective atmosphere, the triflate anion is displaced from the coordination sphere by a water molecule, which is connected to the triflate anion through H-bonds (see Figure 3, bottom). This substitution does not induce any significant change in the coordination bonds and angles (Table S5). Such mono aqua complex was described in the salen series only when the ligand contains several mesityl substituents,[17] otherwise the iron center is hexacoordinated. No

crystals suitable for X-ray diffraction could be obtained from solutions in coordinating solvents such as MeCN or THF, which may be explained by the inability of these molecules to develop hydrogen bonds with the triflate counter anion when they act as a ligand.

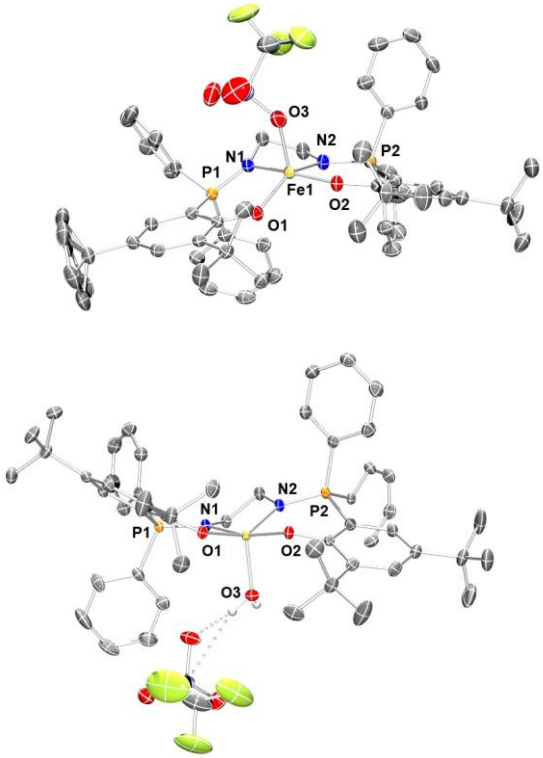

Figure 3. Ortep plot of **[Fe^{III}(Psalen)(OTf)]** (top) and **[Fe^{III}(Psalen)(H$_2$O)](OTf)**: (bottom) most hydrogen atoms and solvent molecules were omitted for clarity

Single crystals of the Fe^{II} complex were obtained from slow evaporation of concentrated acetonitrile or toluene solution. The structure obtained from acetonitrile is presented in Figure 4 while that from toluene can be found in the Supporting Information (Figure S1).

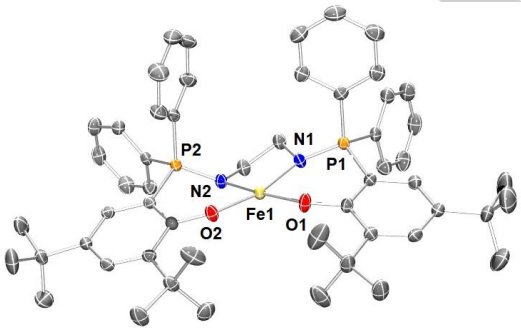

Figure 4. Ortep plot of **[Fe^{II}(Psalen]:** hydrogen atoms and solvent molecules were omitted for clarity

Those structures are highly similar and evidence an almost square planar geometry. No coordination of an apical ligand was observed even in presence of a coordinating solvent. The τ_4 index[18] was calculated at 0.141 which is consistent with a slight distortion from planarity (τ_4 = 0 for square-planar, and τ_4 = 1 tetrahedral geometry). The lengths of the PN bonds (1.60 Å on average) are in line with those previously observed for Fe^{II} complexes.[19]

Compared to Fe^{III} complexes, elongated coordination bonds are expected due to the increased electron density at the metal center. However, this is not so obvious when comparing bond distances in **[Fe^{III}(Psalen)Cl]** and **[Fe^{II}(Psalen)]**. Indeed, the Fe-N and Fe-O bonds are only hardly longer in Fe^{II} compared to Fe^{III} (Tables S6 and S3-5). Additionally, the PN bonds are rather similar in **[Fe^{III}(Psalen)Cl]** and **[Fe^{II}(Psalen)]** (Tables S3 and S6), while they generally elongate upon oxidation of the metal as observed for nickel, palladium or copper complexes.[2-3] The **[Fe^{II}(Psalen)]** structures observed can also be compared with that of a salen analogue for which the phenolate is unsubstituted.[12] In line with previous observations[2, 3b, 15] the coordination sphere around the metal is more contracted in the salen complex than in the phosphasalen complex (see Table S6). Noteworthy **[Fe^{II}(Psalen)]** was prepared and crystallized in coordinating solvents such as MeCN and THF, but no solvent coordination was observed in the solid-state which may be ascribed to the steric hindrance created by the *tert*-butyl substituents. Indeed, THF coordination was observed for a phosphasalen iron(II) complex exhibiting unsubstituted phenolate rings.[20]

Solution properties

Magnetic properties

The magnetic moment of the iron complexes were measured at 293 K in THF solution using the Evans method. For **[Fe^{III}(Psalen)Cl]**, **[Fe^{III}(Psalen)(NO$_3$)]**, and **[Fe^{III}(Psalen)(OTf)]** magnetic moments of 5.87, 5.71, and 5.72 μ_B respectively were determined which corresponds to high spin Fe^{III} complexes (S=5/2). For **[Fe^{II}(Psalen)]** the value of the magnetic moment at 4.96 μ_B is consistent with a Fe^{II} high spin ground state (S=2). This was rather unexpected because of the square planar geometry found in the solid state. Indeed in such geometry, the d_{x2-y2} orbital is destabilized, according to the crystal field theory, therefore, electronic configurations with low (S=0) or intermediate spin (S=1) are expected. The magnetic moment was also measured in the solid state and confirmed the high spin value (Figure S2), which rules out an effect of the solvent. Such a combination of D_{4h} coordination and HS configuration is encountered in some minerals (gillespite, eudialyte, $SrFeO_2$[21] and $CaFeO_2$,[22] in which crystal packing is argued to enforce the unusual environments). Besides, several molecular Fe^{II} complexes with alkoxide or siloxide ligands were reported to display D_{4h} coordination and HS configuration.[23] These ligands, combining anionic and weak field character, stabilize the unusual environment via electronic effects. More recently, D_{4h} HS Fe^{II} complexes involving mixed amido-alkoxide,[24] imino-pyridine,[25] or pyrrolate-pyridine ligand[26] were also reported. To the best of our knowledge, **[Fe^{II}(Psalen)]** is the first example of a D_{4h} HS complex with a N_2O_2 donor set.

UV-visible spectroscopy

The absorption spectra of the iron phosphasalen complexes and **[Zn(Psalen)]** in acetonitrile are shown in Figure 5. The spectrum of the Zn^{II} complex exhibits a band centred at 326 nm, and two shoulders at 273 and 266 nm. Based on previous reports, the low energy band at 326 nm was tentatively assigned to a π→π* from the phenol moiety,[27] and the shoulders as aminophosphonium centered transitions.[28] The spectrum of any $Fe^{II/III}$ complex displays similar intra-ligand transitions with the maximum of the phenol π→π* band (around 300 nm) and three shoulders shifted to higher energies compared to the spectrum of **[Zn(Psalen)]**, but also an additional broad band assigned as a LMCT phenolate→$Fe^{II/III}$ with a maximum between 406 and 497 nm. When compared to the UV-vis spectra of **[Fe^{III}(salen)]** complexes,[17, 29] the LMCT are observed at lower wavelength for the **[Fe^{III}(Psalen)]** complexes in agreement with the electron enriched character of metal centers when linked to two iminophosphorane instead of two imines.

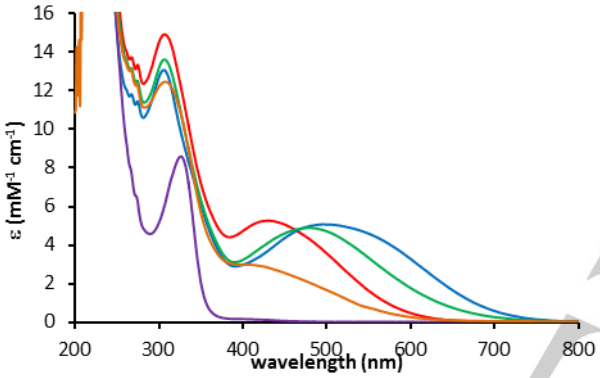

Figure 5. UV-vis spectra of **[Fe^{III}(Psalen)Cl]** (red), **[Fe^{III}(Psalen)(NO_3)]** (green), **[Fe^{III}(Psalen)(OTf)]** (blue), **[Fe^{II}(Psalen)]** (orange/brown) and **[Zn(Psalen)]** (purple) recorded in acetonitrile at 50 µM.

Consistently, it appears that the LMCT energy decreases in the order **[Fe^{II}(Psalen)]** > **[Fe^{III}(Psalen)Cl]** > **[Fe^{III}(Psalen)(NO_3)]** > **[Fe^{III}(Psalen)(OTf)]**. However, the UV-vis spectrum of **[Fe^{III}(Psalen)(OTf)]** recorded in toluene displays a LMCT maximum at higher energy compared to that recorded in MeCN (toluene: λ_{max}=458 nm; MeCN: λ_{max}=497 nm) (Figure 10, compare black and blue traces). Based on this observation, it can be concluded that the OTf^- anion remains bound to the Fe^{III} centre in non-coordinating solvent, as observed in the solid-state (Figure 3). In contrast, the anion is substituted by a solvent molecule in MeCN, thus forming **[Fe^{III}(Psalen)(MeCN)](OTf)**. Therefore, it follows that the LMCT energy decreases in the order **[Fe^{II}(Psalen)]** > **[Fe^{III}(Psalen)Cl]** > **[Fe^{III}(Psalen)(NO_3)]** > **[Fe^{III}(Psalen)(MeCN)](OTf)**, which correlates with an increase of the electron-accepting character of the iron center (Fe^{II}<Fe^{III}) as well as with the electron-donating ability of the exogenous ligand.

Cyclic voltammetry

Cyclic voltammetry experiments have been performed in acetonitrile for all iron(III) complexes as well as zinc(II) compound for comparison purpose. The latter exhibits no redox event on the cathodic scan, but four oxidation waves at 0.77, 0.99, 1.29, and 1.67 V *vs* SCE on the anodic scan (Figure S3) associated to re-reduction peaks of lower intensity at 0.74, 0.91, 1.25, and 1.57 V. The two first pseudo-reversible oxidation processes are consistent with the successive oxidation of the two Zn^{II}-bound phenolate groups into phenoxyl radicals. The two oxidation waves at 1.29 and 1.67 V, that are almost irreversible should correspond to the oxidation of the two iminophosphorane moieties into aminophosphonium cation radical.[30]

The Fe^{III} complexes all display three or four oxidation processes, that take place at higher potentials compared to their Zn^{II} analogue in agreement with a greater Lewis acidity for iron(III) (Figure S3). However, their precise assignment is difficult due to partial overlap. Of note, the potential value of the first oxidation is dependent on the donating ability of the exogenous ligand. Indeed, this potential value increases with lower electron density at the metal center; following the order **[Fe^{III}(Psalen)Cl] < [Fe^{III}(Psalen)(NO_3)] ≈ [Fe^{III}(Psalen)(MeCN)]$^+$** (formed from **[Fe^{III}(Psalen)(OTf))]** in MeCN, *vide supra*). Noteworthy, the reversibility of the first oxidation process can be increased upon increase of the scan rate (Figure S4).

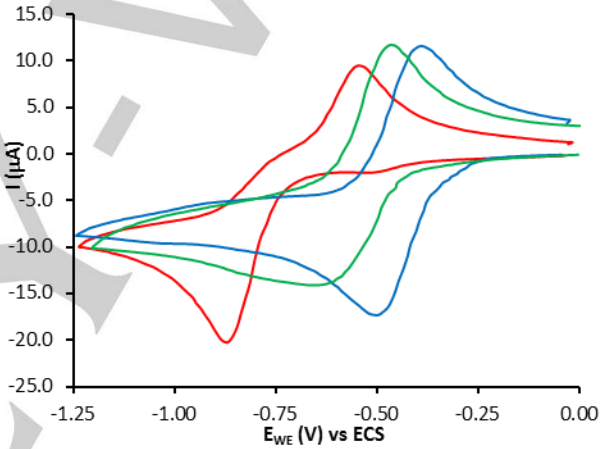

Figure 6. Cylic voltammograms of the reduction of **[Fe^{III}(Psalen)Cl]** (red), **[Fe^{III}(Psalen)(NO_3)]** (green), **[Fe^{III}(Psalen)(OTf)]** (blue) recorded in acetonitrile (containing 100 mM Bu_4NPF_6 and 1.6 mM of complex) at a glassy carbon electrode (scan rate 100 mV s^{-1}).

On the cathodic scan, an additional process corresponding to the Fe^{III}/Fe^{II} couple is observed for the iron(III) complexes (Figure 6). Overall, the Fe^{III}/Fe^{II} reduction peaks are observed at potential values, which are in agreement with the relative electron-donating ability previously established: the reduction is all the more difficult that the exogenous ligand is electron-donating. For **[Fe^{III}(Psalen)(MeCN)]$^+$**, a reversible redox process centred at -0.44 V is observed. **[Fe^{III}(Psalen)(NO_3)]** displays a quasi-reversible process centred at -0.55 V with a reduction half-wave slightly broadened. In contrast, an irreversible process is observed for **[Fe^{III}(Psalen)Cl]**, with a Fe^{III}-to-Fe^{II} reduction peak at -0.88 V and an oxidation peak at -0.51 V on the reverse scan. This 0.37 V difference between the cathodic and anodic processes can be interpreted as an ECE mechanism. Reduction of Fe^{III}Cl at -0.88 V, is followed by a release of the chloride anion yielding an Fe^{II} species which is oxidized at -0.51 V. In such cases, recording the CV at higher scan rate might allow to bypass partially or completely the chemical reaction and thus increasing the reversibility of the EC process. Upon increasing the scan rate up to 5 V s^{-1} (Figure S5), the cathodic process in

the CV of **[Fe^{III}(Psalen)Cl]** remains firmly irreversible and the peak separation increases with the scan rate (as expected for a diffusion-limited process). This suggests that the **[Fe^{II}(Psalen)Cl]**$^-$ complex is highly unstable, and that the chloride removal is completed in less than 0.2 second.

The Fe^{III}/Fe^{II} reduction potential of the Psalen complexes are ~0.4-0.5 V lower compared to their salen analogues,[31] thus confirming the tendency previously described. Complexes with such low Fe^{III}/Fe^{II} reduction potential are expected to display a poor activity in aerobic oxidation of cyclohexene, based on the correlation established by Gray and co-workers.[31] However, the mechanism for 2-naphthol oxidation described by Katsuki involves the one-electron-oxidation of the [Fe^{III}(Salan)]-naphtholate intermediate as the kinetically-determining step.[10] Using the potential of the first oxidation wave as a reference (assigned as a phenolate to phenoxyl radical oxidation process), we anticipated that **[Fe^{III}(Psalen)]** complexes would be better catalysts for 2-naphthol oxidation compared to their salen analogues. Indeed, the cyclic voltammetry study of the **[Fe^{III}(Psalen)Cl]** complex has a first oxidation half-wave at 1.1 V (*vs* ECS), that is 0.3 V lower compared to that reported for the iron salen complex bearing mesityl substituents reported by Fujii.[29] On the other hand, this potential is ~0.2 V higher compared to the first oxidation half-wave reported by Katsuki and co-workers[32] for their iron salan derivatives.

EPR spectroscopy

EPR measurements were recorded at low temperature (10 K) on powder samples and on frozen solutions using either non-coordinating (toluene) or coordinating solvent (MeCN). The first-derivative spectrum recorded for the **[Fe^{III}(Psalen)Cl]** powder sample displays resonances with g-values of 9.1, 5.2, 3.5, 2.8, (set 1) and other ill-defined signals at higher field (Figure 7). This spectrum is typical for a high spin Fe^{III} (S=5/2) species with E/D of 0.17. EPR spectra of this complex dissolved in CH_2Cl_2/toluene or CH_2Cl_2/MeCN display signals similar to the set 1 observed from the powder sample (CH_2Cl_2/toluene: g = 8.9, 5.2, 3.5, 2.3; CH_2Cl_2/MeCN: g = 8.9, 5.0, 3.8), as well as an additional signal with g = 4.3 characteristic of a rhombic species (E/D = 0.33).

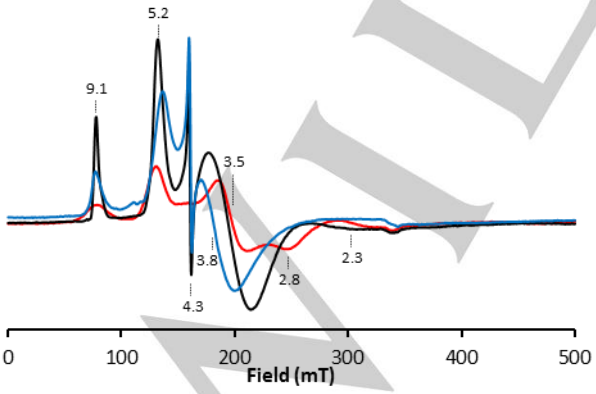

Figure 7. EPR spectra of **[Fe^{III}(Psalen)Cl]** as powder (red), in CH_2Cl_2/Toluene (black**),** and in CH_2Cl_2/CH_3CN (blue)**.**

Therefore, we propose that the set of signals with E/D = 0.17 accounts for the solid-state structure described above. However, the resonance at g = 4.3 probably arises from a chemical modification of the initial complex in solution (resonances at g = 4.3 are ubiquitous in EPR of Fe^{III} species, and therefore provide little structural information).

For the complex **[Fe^{III}(Psalen)(NO$_3$)]**, the spectrum recorded on the powder sample displays a main signal at g = 4.3, consistent with the presence of one species with E/D = 0.33 (Figure 8). In acetonitrile or toluene, the spectrum of this complex also displays the signal at g = 4.3. Nonetheless, the resonance appears sharper in toluene. Therefore, the species present in solution might correspond to the structure of **[Fe^{III}(Psalen)(NO$_3$)]** characterized by X-ray diffraction, in which a hexavalent iron(III) ion is coordinated by a bidentate NO_3 ligand. This is rather unexpected that the nitrate ion binds so tightly to the Fe^{III} center even in acetonitrile.

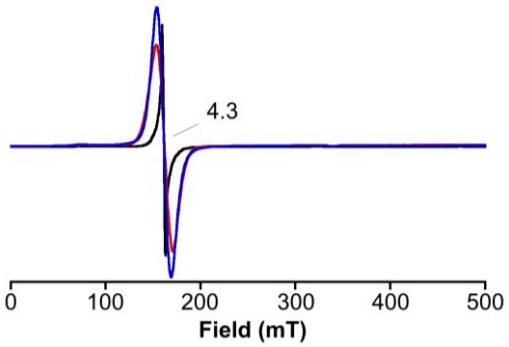

Figure 8. EPR spectra of **[Fe^{III}(Psalen)(NO$_3$)]** as powder (red), in toluene (black**),** and in acetonitrile (blue).

The spectrum recorded on powder **[Fe^{III}(Psalen)(OTf)]** displays a main signal at g = 4.3 which remains but becomes sharper upon dissolution in toluene (Figure 9). In contrast, the spectrum recorded for an acetonitrile solution of **[Fe^{III}(Psalen)(OTf)]** displays new resonances at g = 8.1, 5.6, 2.8, 1.8, and ill-defined signals at higher field (set 2), while the signal at g = 4.3 is retained. The set 2 is consistent with the presence of a more axial species with E/D = 0.10. We propose that the species with E/D = 0.33 observed in the powder and in toluene solution corresponds to the complex characterized by X-ray diffraction (*i.e*. with the triflate coordinated to iron).

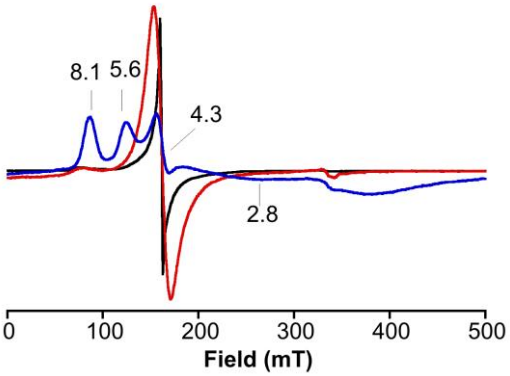

Figure 9. EPR spectra of **[Fe^{III}(Psalen)(OTf)]** as powder (red), in toluene (black**),** and in acetonitrile (blue).

Upon dissolution in acetonitrile, at least one solvent molecule displaces the triflate anion, thus leading to the new species **[Fe^{III}(Psalen)(MeCN)]$^+$** with E/D = 0.10.

In order to strengthen these assignments, an excess of pyridine (2% v/v), a better Lewis base than acetonitrile, was added to the solution of the different Fe^{III} complexes in acetonitrile. Under these conditions, the spectra of **[Fe^{III}(Psalen)Cl], [Fe^{III}(Psalen)(NO$_3$)] and [Fe^{III}(Psalen)(MeCN)]$^+$** become similar (Figure S8). All spectra include signals with g = 8.5, 5.4, and a broad one at 3.2-3.1, which are similar to those of set 2. Additionally, they all exhibit a minor signal at g = 4.3. Again, set 2 indicates the presence of an almost axial species with E/D = 0.10, as for **[Fe^{III}(Psalen)(OTf)]** in acetonitrile. Therefore, we propose that this species can be formulated as **[Fe^{III}(Psalen)(py)]$^+$** or **[Fe^{III}(Psalen)(py)$_2$]$^+$.**

Having established that acetonitrile can substitute the triflate anion but not the nitrate or the chloride, we wondered if the chloride could substitute the nitrate anion. One equivalent of NBu_4Cl was added to EPR tubes containing an acetonitrile solution of **[Fe^{III}(Psalen)Cl]**, **[Fe^{III}(Psalen)(NO$_3$)]** or **[Fe(Psalen)(MeCN)]$^+$**. As expected, the spectrum of **[Fe(Psalen)Cl]** remains unchanged (Figure S9). In contrast, the spectra of **[Fe(Psalen)(NO$_3$)]** and **[Fe(Psalen)(MeCN)]$^+$** displayed the development of signals at g = 8.9, 5.2, *ca.* 3.5 (broad), corresponding to set 1 (see above). Overall, this observation is consistent with formation of **[Fe^{III}(Psalen)Cl]**. Therefore, the chloride added is able to substitute both the acetonitrile and the nitrate exogenous ligands. Hence, these EPR measurements allow establishing the following order for the axial ligand lability in **[Fe^{III}(Psalen)] complexes** : $OTf^- > CH_3CN > NO_3^- > Cl^-$.

Catalytic 2-naphthol coupling

The reaction was performed using dioxygen as oxidant under the conditions described by Katsuki and co-workers[9] with the three **[Fe^{III}(Psalen)(X)]** complexes (Table 1, Entry 1, 2, 3). Under these conditions, the 3 complexes display a modest catalytic activity, with a slightly better performance observed for the **[Fe^{III}(Psalen)(OTf)]** complex, which contains the more labile exogenous ligand. Along this line, no product was obtained when the reaction was performed in acetonitrile (Entry 4), this solvent was shown to compete with 2-naphthol for coordination to the metal center (*vide infra*). As expected, no conversion was obtained in the absence of O_2 (entry 5). No conversion was obtained either when [Fe(OTf)$_3$] was used as catalyst (Entry 6). The Katsuki catalyst is a [Fe^{III}(salan)(μ-hydroxo)]$_2$ dimer, which dissociates upon 2-naphthol binding into two salan Fe^{III}-naphtholate monomer. The catalyst loading reported is based on the dimer (4 mol% dimer = 8 mol% monomer). Therefore, the reaction was repeated using 8 mol% loading of **[Fe^{III}(Psalen)(OTf)]** which resulted in a *ca.* two fold increase of the yield (18%, entry 7). Nonetheless, this result is lower than that reported for the Katsuki catalyst under similar conditions (entry 8). This order of reactivity is consistent with the mechanism proposed and the easier oxidation of salan complexes compared to Psalen ones. The reactions were repeated with 4-fold increased concentrations, while retaining the same catalyst loading (entry 9-14). As expected, the yield improved with the concentration (entry 11-15). Surprisingly, the highest yield was obtained for the **[Fe^{III}(Psalen)Cl]** rather than **[Fe^{III}(Psalen)(OTf)]** complex. This suggests that high concentrations are required to allow the coordination of naphthol to the Fe^{III} center, even for the **[Fe^{III}(Psalen)Cl]**. Following Katsuki's mechanism, this latter is expected to be a better catalysts due to its lower redox signature (see above).

Table 1. 2-naphthol coupling catalyzed by **[Fe(Psalen)] complexes**.

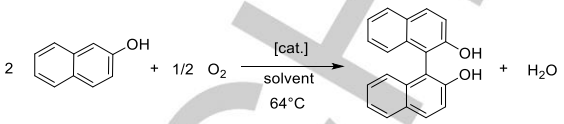

Entry	catalyst	[cat] mM	mol% cat.	Atm.	solvent	Yield %[a]
1	**[Fe(Psalen)Cl]**	4	4	air	toluene	7
2	**Fe(Psalen)(NO$_3$)]**	4	4	air	toluene	8
3	**[Fe(Psalen)(OTf)]**	4	4	air	toluene	11
4	**[Fe(Psalen)(OTf)]**	4	4	air	MeCN	0
5	**[Fe(Psalen)(OTf)]**	4	4	argon	toluene	0
6	**[Fe(OTf)$_3$]**	4	4	air	toluene	0
7	**[Fe(Psalen)(OTf)]**	8	8	air	toluene	18
8[b]	**[Fe(salan)-υ-(OH)]2**[b]	8[b]	8[b]	air[b]	toluene[b]	87[b]
9	**[Fe(Psalen)Cl]**	16	4	air	toluene	45
10	**[Fe(Psalen)(NO$_3$)]**	16	4	air	toluene	23
11	**[Fe(Psalen)(OTf)]**	16	4	air	toluene	34
12	**[Fe(Psalen)(OTf)]**	16	4	air	MeCN	0
13	**[Fe(Psalen)(OTf)]**	16	4	argon	toluene	0
14	**[Fe(OTf)$_3$]**	16	4	air	toluene	3
15	**[PsalenFe(OTf)]**	32	8	air	toluene	51

The reactions were performed at 64°C for 72 h on the 0.1 (entry 1-7) or 0.2 mmol scale (entry 9-15). [a] Determined by ^{1}H NMR using 1,3,5-trimethoxybenzene as internal standard. [b] from reference [9], performed at 60°C.[9]

Aiming to demonstrate the binding of substrate with **[Fe^{III}(Psalen)(X)]** complexes, additions of increasing amounts of 2-naphthol to the solutions of **[Fe^{III}(Psalen)(OTf)]** in either toluene or MeCN were monitored by UV-vis (Figure 10). Spectral evolutions are consistent with quantitative substitution of the OTf^- ligand by excess 2-naphthol in toluene. In MeCN the change is less pronounced suggesting competition with the solvent.

Then, we studied the electrochemical oxidation of **[Fe^{III}(Psalen)(MeCN)]$^+$** in the presence and the absence of 2-naphthol. Interestingly, the first oxidation half-wave for **[Fe^{III}(Psalen)(MeCN)]$^+$** undergoes a slight (0.06 V) cathodic shift upon the addition of 5 equivalents of 2-naphthol but the process is partially overlapped with that for the direct substrate oxidation at the electrode (Figure S6). As for the UV-vis study, we repeated this measurement in a non-coordinating solvent (CH_2Cl_2) in order to maximize the 2-naphtholate coordination to the iron center. In CH_2Cl_2, the first oxidation half-wave for the

[Fe^{III}(Psalen)(OTf)] complex undergoes a larger cathodic shift (0.25 V) upon the addition of 5 equivalents substrate (Figure S7). In both solvents, the addition of substrate is associated with a slight current increase of the first oxidation half-wave. Additionally, anodic signal appears at 0.7-0.8 V. While it is difficult to assign this process, its potential suggests it may be associated with a bis coordination of 2-naphthol.

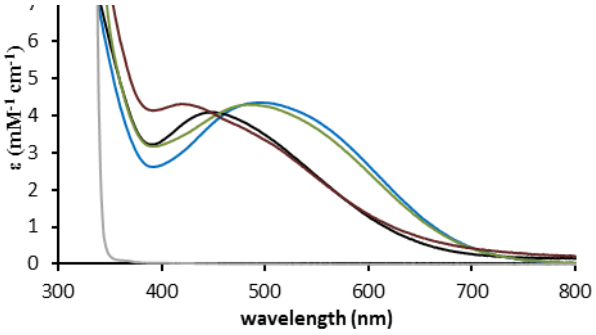

Figure 10. UV-vis spectra of 1 mM **[Fe(Psalen)(OTf)]** recorded either in the absence (— MeCN ; — Toluene) or the presence of 25 mM 2-naphthol (— MeCN ; — Toluene) in 1 mm pathlength cuvette. Control spectra recorded for 25 mM 2-naphthol recorded in toluene (—); the spectrum recorded in MeCN was overlapped.

Overall, these measurements indicate that 2-naphthol oxidation occurs at a lower potential when it is coordinated to the **[Fe^{III}(Psalen)]** complex. However, the catalytic steps following this oxidation are slow on the CV timescale since no electrocatalytic wave is observed. In the electrochemical study by Katsuki and co-workers,[32] interpretations of the electrochemical response upon 2-naphthol addition were complicated by monomer-dimer equilibria. Therefore, our study constitutes the first electrochemical evidence of 2-naphthol oxidation promoted by iron salen derivatives.

Conclusion

Phosphasalen Fe^{III} complexes differing by the nature of the fifth ligand (Cl, NO_3, OTf) and a square planar Phosphalen Fe^{II} complex have been synthesized and characterized both in the solid state and in solution. All of these complexes contain a high spin iron centre even the square planar Fe^{II} complex. UV-vis spectroscopy and electrochemistry confirm that the electron density at the metal center decreases following the order **[Fe^{II}(Psalen)]** > **[Fe^{III}(Psalen)Cl]** > **[Fe^{III}(Psalen)(NO$_3$)]** ≈ **[Fe^{III}(Psalen)(OTf)]** > **[Fe^{III}(Psalen)(MeCN)](OTf).** The low reduction potential measured for the Fe^{III}/Fe^{II} prompted us to investigate the oxidative coupling of 2-naphtol which was previously described with salan based iron(III) complexes. Up to 50 % conversion was obtained for catalysis conducted in toluene with O_2 from air at 8 mol % catalyst loading. The interaction between naphtol and the Fe^{III} complex was studied by cyclic voltammetry and UV-vis spectroscopy and evidences the formation of the [Fe(Psalen)($C_{10}H_7O$)] complex. The catalytic performances of these iron phosphasalen complexes could probably be improved by fine-tuning of the ligand structure. Studies in that direction are currently ongoing in our laboratories.

Experimental Section

General considerations. All experiments were performed under an inert atmosphere using either a schlenk line and/or a MBraun MB-Unilab Pro SP glove box with an Ar atmosphere containing [O_2] < 0.1 ppm and [H_2O] < 0.1 ppm. Anhydrous solvents were purified on a MBraun MB-SPS 800 solvent purification machine. Anhydrous and degassed solvents were additionally degased by 3 successive freeze/vacuum/thaw cycles and then cryodistilled on a vacuum line equipped with Young valves. [$FeCl_2(THF)_{1.5}$] was prepared according to published method.[33] Bu_3N and ethylene diamine were distilled and KH 30% in mineral oil was washed with pentane and dried in vacuo prior to use. All other reagents were used as purchased. The Phosphasalen ligand was synthesized as previously described.[12]

Nuclear magnetic resonance (NMR) spectra were recorded at 293 K on a Avance III 300 Bruker spectrometer operating at 300 MHz for ^{1}H, 75.5 MHz for ^{13}C, 121.5 MHz for ^{31}P. Solvent peaks were used as internal references for ^{1}H and ^{13}C chemical shifts (ppm). ^{31}P peaks were referenced to external 85 % H_3PO_4. The following abbreviations are used: b, broad; s, singlet; d, doublet; t, triplet; q, quartet; m, multiplet. NMR spectra were analyzed using the MestReNova software. The labelling for **[Zn(Psalen]** is indicated in Figures S. Evans' analyses were run in NMR tubes equipped with either screw-capped or young valve containing ~10 mg of product dissolved in 1 mL of deuterated solvent. NMR spectra were recorded before and after the addition of the capillaries containing the deuterated solvent alone. The magnetic susceptibility was calculated from the shift of the solvent peaks as previously reported. [34] Magnetic moments (μ) are reported in units of Bohr magneton (μB).

X-band EPR spectra were recorded on a Bruker ELEXSYS 500 spectrometer equipped with a Bruker ER 4116DM X band resonator, an Oxford Instrument continuous flow ESR 900 cryostat, and an Oxford ITC 503 temperature control system. The parameters were as follow T=10 K, MW freq. = 9.636 GHz, MW power = 1.0 mW, MA = 8 Gauss, Mod. Freq = 100 KHz, Gain = 38 db. For the addition of 2-naphthol to **[Fe(Psalen)(OTf)]**, the gain was set to 44G.

Mass spectrometry experiments were performed on a tims-TOF mass spectrometer (Bruker, France). ESI (ElectroSpray Ionisation) source has been used in positive or negative mode according to the structure of the compound studied. Samples were prepared in acetonitrile and introduced at a 5 μL min^{-1} flow rate into the interface of the instrument. Capillary and end plate voltages were set at 4.5 kV and 0.5 kV. Nitrogen was used as the nebulizer and drying gas at 2.5 bar and 3 Lmin^{-1}, respectively, with a drying temperature of 180°C and with a drying and vaporizer temperatures of 220°C. Tuning mix (Agilent, France) was used for calibration. The elemental compositions of all ions were determined with the instrument software Data Analysis, the precision of mass measurement was less than 5 ppm.

Elemental analyses were obtained from the London Metropolitan University (London, United-Kingdom).

UV-vis measurements were recorded on a CARY 60 spectrometer from Agilent Technologies using quartz cuvette of 1 cm pathlength (unless otherwise stated). A cuvette equipped with a young valve was used to record the spectra of **PSalen** and **[Fe(Psalen)]**. The wavelengths of the maxima are reported in nm and their respective extinction coefficients are reported in bracket using L mol^{-1} cm^{-1} as unit. Shoulders are denoted as sh, and broad bands as br. For the titration of **[Fe(Psalen)(OTf)]** with 2-naphthol, 1 mM solution of complex in MeCN or toluene were added to 1 mm pathlength cuvette and a 200 mM solution of 2-naphthol was added portion-wise. The absorbance of the spectra was corrected for dilution.

Cyclovoltammograms of solutions containing generally 1.6 mM complex and 100 mM Bu_4NPF_6 in MeCN were recorded using a three electrode setup including: a vitreous carbon working-electrode, a platinum counter-electrode and an SCE reference electrode. The working electrode was polished on Mecaprex disc after each scan and subsequently cleaned with ethanol. The potentials were internally referenced to the Fc$^+$/Fc couple by addition of ferrocene in the electrochemical cell but are displayed versus SCE using the conversion value 0.39 V. Unless otherwise stated, the scan rate was set to 100 mV/s.

UNCORRECTED PROOF

Cyclovoltammograms are recorded with the following sequence of potentials: 0 → -2.0 → +2.0 → 0 V, or 0 → -1.2 → 0 V.

Suitable crystals for X-Ray analysis of **[Fe(Psalen)Cl]**, **[Fe(Psalen)(OTf)]**, and **[Fe(Psalen)]** were mounted in inert oil onto a kapton loop and placed in a cold stream of nitrogen. Data were collected at 150 K on a Bruker Kappa APEX II diffractometer using a Mo-κ (λ = 0.71069 Å) X-ray source and a graphite monochromator. The crystal structures were solved using SIR 97[35] and refined in SHELXL-97 and SHELXL-2014[36] by full-matrix least-squares using anisotropic thermal displacement parameters for all non-hydrogen atoms. Hydrogen atoms were placed either at geometrically calculated positions or according to the localization of electronic densities around the carbon atoms. ORTEP drawings were made using ORTEP III[37] for Windows. X-ray diffraction data for compounds **[Fe(Psalen)(NO_3)]** and **[Fe(Psalen)(H_2O)(OTf)]** were collected on a VENTURE PHOTON100 CMOS Bruker diffractometer with Micro-focus IuS source Cu Kα radiation. Crystals were mounted on a CryoLoop (Hampton Research) with Paratone-N (Hampton Research) as cryoprotectant and then flashfrozen in a nitrogen-gas stream at 100 K. The temperature of the crystal was maintained at the selected value by means of a 700 series Cryostream cooling device to within an accuracy of ±1K. The data were corrected for Lorentz polarization, and absorption effects. The structures were solved by direct methods using SHELXS-97[36] and refined against F^2 by full-matrix least-squares techniques using SHELXL-2018[38] with anisotropic displacement parameters for all non-hydrogen atoms. Hydrogen atoms were located on a difference Fourier map and introduced into the calculations as a riding model with isotropic thermal parameters. All calculations were performed by using the Crystal Structure crystallographic software package WINGX.[39]

Syntheses. *Synthesis of [Zn(Psalen)]:* in the glove box, the ligand **Psalen** (100 mg, 0.110 mmol) is dissolved in the minimal amount of THF and the solution is transferred to a 100 mL Schlenk tube. Then, $ZnBr_2$ (25 mg, 0.110 mmol) also dissolved in the minimum amount of THF is added to the Schlenk tube. The solution is stirred at room temperature for two hours, after which ^{31}P NMR was run and a single peak at 35.3 ppm was observed. The suspension is transferred to a tube, centrifuged for 1 hour, the white solid is discarded, and the solution is dried in high vacuum to obtain **[Zn(Psalen)]** as a white powder (69 mg, 70%). ^{1}H NMR (CD_2Cl_2, 300 MHz): 7.63 (m, 8H, H_{12}), 7.55 (dd, $^3J_{H,H}$ = 7.5 Hz, $^4J_{H,-H}$ = 1.7 Hz, 4 H, H_{14}), 7.48 (m, 8H, H_{13}), 7.37 (d, $^4J_{H,H}$ = 2.5 Hz, 2H, H_4), 6.53 (dd, $^4J_{H,H}$ = 2.5 Hz, $^4J_{P,H}$ = 16.0, H^6), 2.97 (m, 4H, H_{15}), 1.26 (s, 18H, H_8), 1.08 (s, 18H, H_{10}); ^{13}C{^{1}H}NMR (CD_2Cl_2, 75.5 MHz): 171.7 (C_2), 141.7 (C_3), 134.5 (C_5), 133.4 (C_{13}), 132.1 (C_{14}), 130.0 (C_{11}), 128.9 (C_4), 128.8 (C_{12}), 128.1 (C_6), 108.5 (C_1), 48.5 (C_{15}), 35.4 (C_7), 33.9 (C_9), 31.3 (C_{10}), 29.5 (C^8). ^{31}P{^{1}H} NMR (CD_2Cl_2, 121.5 MHz): 35.2. ESI-MS (M = $C_{54}H_{64}Br_2N_2O_2P_2Zn$): 899.38 ([M+H]$^+$, 23%), 837.47 ([M-Zn+3H]$^+$, 100%), 405.22 ([$C_{26}H_{32}NOP$]$^+$, 17%). HRMS: calculated for [$C_{54}H_{65}N_2O_2P_2Zn$]$^+$ ([M+H]$^+$): 899.3813; found: 899.3831. UV-vis (MeCN): 326 (8600), 273 (sh, 6550), 266 (sh, 8000).

Synthesis of [Fe(Psalen)]: in the glove box, the ligand **Psalen** (107 mg, 0.117 mmol) is dissolved in the minimal amount of THF and the solution is transferred to a 100 mL Schlenk tube. Then, [$FeCl_2(THF)_{1.5}$] (28 mg, 0.117 mmol) also dissolved in the minimum amount of THF is added to the Schlenk tube. The solution is stirred at room temperature for two hours, after which the suspension is filtered, and the solution is dried in high vacuum to afford **[Fe(Psalen)]** as a pink solid (60 mg, 58 %). Crystals for X-ray diffraction were grown by evaporation from a solution in Toluene. Evans method (C = 9.6 mM; THF-d_8): 4.96 μ_B, S = 2. UV-vis (MeCN): 406 (br, 3000), 305 (12450), 273 (sh, 12250), 267 (sh, 13050), 259 (sh, 13600). Elemental analysis calculated for $C_{54}H_{64}Cl_{0.5}FeK_{0.5}N_2O_2P_2$ ($PSalenFe^{II}$.0.5KCl): C 69.88, H 6.95, N 3.02, found C 69.96, H 6.84, N 3.00. This compound was also prepared by a similar method using MeCN as solvent and [$Fe(OTf)_2(MeCN)_2$]. Crystals suitable for X-ray diffraction were grown by evaporation from a solution in MeCN. The coordination sphere from this complex was similar to the one prepared by the other method.

Synthesis of [Fe(Psalen)Cl] : in the glove box, the ligand **Psalen** (200 mg, 0.219 mmol) is dissolved in the minimal amount of THF and the solution is transferred to a 100 mL Schlenk tube. Then, $FeCl_3$ (36 mg, 0.219 mmol) also dissolved in the minimum amount of THF is added to the Schlenk tube. The solution is stirred at room temperature for two hours, after which no signal could be observed by ^{31}P NMR monitoring. The suspension is transferred to a tube, centrifuged, the white solid is discarded, and the solution is dried in high vacuum. The solid residue is washed with 2x10 mL pentane and then dried in high vacuum again to obtain **[Fe(Psalen)Cl]** as a red powder (110 mg, 54%). Crystals for X-ray diffraction were grown by evaporation from a solution in dichloromethane. Evans method (C = 10.8 mM; THF-d_8): 5.87 μ_B, S = 5/2. UV-vis (MeCN): 428 (br, 5270), 307 (14920), 275 (sh, 13340), 267 (sh, 13280), 258 (sh, 14500). ESI-MS (M = $C_{54}H_{64}ClFeN_2O_2P_2$): 1004.37 (10%), 926.35 ([M+H]$^+$, 100%), 890.38 ([M-Cl]$^+$, 56%), 406.23 (15%). HRMS: calculated for [$C_{54}H_{64}FeN_2O_2P_2$]$^+$ ([M-Cl]$^+$): 890.3787; found: 890.3794. Elemental analysis calculated for $C_{54}H_{64}ClFeN_2O_2P_2$ [Fe(Psalen)Cl]: C 70.01, H 6.96, N 3.02, found C 69.93, H 7.07, N 2.93.

Synthesis of [Fe(Psalen)(NO_3)]: in the glove box, the ligand **Psalen** (300 mg, 0.329 mmol) is dissolved in the minimal amount of THF and the solution is transferred to a 100 mL Schlenk tube. Then, $Fe(NO_3)_3.9H_2O$ (133 mg, 0.329 mmol) also dissolved in the minimum amount of THF is added to the Schlenk tube. The solution is stirred at room temperature for two hours, after which no signal could be observed by ^{31}P NMR monitoring. The suspension is transferred to a tube, centrifuged, the white solid is discarded, and the solution is dried in high vacuum. The solid residue is washed with 2x10 mL pentane and then dried in high vacuum again to obtain **[Fe(Psalen)(NO_3)]** as a red powder (200 mg, 64%). Crystals for X-ray diffraction were grown by evaporation from a solution in THF. Evans method (C = 10.6 mM; THF-d_8): 5.71 μ_B, S = 5/2. UV-vis (MeCN): 480 (br, 5200), 307 (14400), 274 (sh, 13200), 267 (sh, 13900), 261 (sh, 14400). ESI-MS (M = $C_{54}H_{64}FeN_2O_2P_2^+$): 953.37 ([M+$NO_3$+H]$^+$, 3%), 926.36 ([M+Cl+H]$^+$, 100%), 890.38 ([M]$^+$, 60%). HRMS: calculated for [$C_{54}H_{64}FeN_2O_2P_2$]$^+$ ([M]$^+$): 890.3787; found: 890.3789. Elemental analysis calculated for $C_{54}H_{70}FeN_3O_8P_2$ ([Fe(Psalen)(NO_3)].3H_2O): C 65.22, H 6.85, N 4.08, found C 65.23, H 6.81, N 4.07.

Synthesis of [Fe(Psalen)(OTf) : in the glove box, the ligand **Psalen** (400 mg, 0.438 mmol) is dissolved in the minimal amount of MeCN and the solution is transferred to a 100 mL Schlenk tube. Then, [$Fe(OTf)_3$] (220 mg, 0.438 mmol) also dissolved in the minimum amount of MeCN is added to the Schlenk tube. The solution is stirred at room temperature for 2 hours, after which no signal could be observed by ^{31}P NMR monitoring. The reaction mixture is then dried in high vacuum. The solid residue is washed with 2x10 mL pentane and then dried in high vacuum again to obtain **[Fe(Psalen)(OTf)]** as a dark-red powder (363 mg, 80%). Crystals suitable for X-ray diffraction were grown by evaporation from a solution of cyclohexane in the glove box. Crystals of the hydrated complex, [Fe(Psalen)(OTf)(H_2O)] were obtained upon aerobic evaporation of a solution in toluene. Evans method (C = 10.8 mM; THF-d_8): 5.72 μ_B, S = 5/2. UV-vis (MeCN): 497 (br, 5100), 306 (13050), 275 (sh, 11450), 267 (sh, 11800), 262 (sh, 12000). ESI-MS (M = $C_{54}H_{64}FeN_2O_2P_2^+$): 926.36 ([M+Cl+H]$^+$, 13%), 890.38 ([M]$^+$, 26%), 837.47 ([M-Fe+3H]$^+$, 31%), 449.27 (100%). HRMS: calculated for [$C_{54}H_{64}FeN_2O_2P_2$]$^+$ ([M]$^+$): 890.3787; found: 890.3811. Elemental analysis calculated for $C_{55}H_{64}F_3FeN_2O_5P_2S$ ([Fe(Psalen)(OTf)]): C 63.52, H 6.20, N 2.69, found C 63.19, H 5.89, 2.53.

General procedure for the 2-naphthol coupling reaction For the reaction at 4 mM catalyst and 100 mM, 2-naphthol (4 mol% loading), the iron catalyst (FeCl: 3.7 mg ; $FeNO_3$: 4.0 mg ; FeOTf : 4.2 mg ; [$Fe(OTf)_3$] : 2.0 mg, 4 μmol) and 2-naphthol (14.4 mg, 100 μmol) were poured into a 5 mL flask and dissolved in toluene or MeCN (1 mL). The reaction was stirred and heated (bath temperature : 64°C) for 3 days using a cooler in order to avoid evaporation of the solvent. At this point, the reaction mixture was dried in vacuo and then purified on a short SiO_2 plug using a pentane/Et_2O (2/1) eluent. The starting material and the main product (1,1-binol) were collected together and the minor side-products eluting slowly were discarded. The dried fraction was

redissolved in $CDCl_3$ and an aliquot of 1,3,5-trimethoxybenzene solution in $CDCl_3$ was added (50 µL, 420 mM). The yield of recovered product was determined from the ratio of integration for the doublet at 8.1 ppm (1,1-binol) and the singlet at 6.1 ppm (starting material). For the reaction at 16 mM catalyst and 400 mM 2-naphthol (4 mol% loading), 8 µmol of catalyst, 200 µmol of 2-naphthol and 0.5 mL of solvent were used instead. The amount of catalyst was increased 2-fold for the reaction with 8 mol% loading. For the catalytic assays performed under Argon, the reaction mixtures were initially prepared in the glove box and the reactions were performed in a schlenk flask.

Acknowledgements

Eric Riviere is thanked for the magnetic measurements**.** This work is supported by a public grant overseen by the French National Research Agency (ANR) as part of the "Investissements d'Avenir" program (Labex Charmmmat, ANR-11-LABX-0039-grant). CNRS, Ecole polytechnique and Université Paris Saclay are also acknowledged for their financial support.

Keywords: iron • N,O ligands • phosphorus • oxidative coupling • phosphasalen

[1] a) M. Costas, M. P. Mehn, M. P. Jensen, L. Que, *Chem. Rev.* **2004**, *104*, 939-986; b) S. M. Hoelzl, P. J. Altmann, J. W. Kueck, F. E. Kuehn, *Coord. Chem. Rev.* **2017**, *352*, 517-536; c) M. L. Pegis, C. F. Wise, D. J. Martin, J. M. Mayer, *Chem. Rev.* **2018**, *118*, 2340-2391; d) O. Y. Lyakin, K. P. Bryliakov, E. P. Talsi, *Coord. Chem. Rev.* **2019**, *384*, 126-139.

[2] T. P. A. Cao, S. Labouille, A. Auffrant, Y. Jean, X. F. Le Goff, P. Le Floch, *Dalton Trans.* **2011**, *40*, 10029-10037.

[3] a) T. P. A. Cao, G. Nocton, L. Ricard, X. F. Le Goff, A. Auffrant, *Angew. Chem.-Int. Edit.* **2014**, *53*, 1368-1372; b) I. M. Marín, T. Cheisson, R. Singh - Chauhan, C. Herrero, M. Cordier, C. Clavaguéra, G. Nocton, A. Auffrant, *Chem. Eur. J.* **2017**, *23*, 17940-17953.

[4] G. Bringmann, T. Gulder, T. A. M. Gulder, M. Breuning, *Chem. Rev.* **2011**, *111*, 563-639.

[5] E. I. Solomon, U. M. Sundaram, T. E. Machonkin, *Chem. Rev.* **1996**, *96*, 2563-2605.

[6] a) H. Shalit, A. Dyadyuk, D. Pappo, *Journal of Organic Chemistry* **2019**, *84*, 1677-1686; b) M. C. Kozlowski, B. J. Morgan, E. C. Linton, *Chem. Soc. Rev.* **2009**, *38*, 3193-3207.

[7] Y. E. Lee, T. Cao, C. Torruellas, M. C. Kozlowski, *J. Am. Chem. Soc.* **2014**, *136*, 6782-6785.

[8] F. G. Bordwell, J. P. Cheng, *J. Am. Chem. Soc.* **1991**, *113*, 1736-1743.

[9] H. Egami, T. Katsuki, *J. Am. Chem. Soc.* **2009**, *131*, 6082-6083.

[10] H. Egami, K. Matsumoto, T. Oguma, T. Kunisu, T. Katsuki, *J. Am. Chem. Soc.* **2010**, *132*, 13633-13635.

[11] N. Segaud, J. N. Rebilly, K. Senechal-David, R. Guillot, L. Billon, J. P. Baltaze, J. Farjon, O. Reinaud, F. Banse, *Inorg. Chem.* **2013**, *52*, 691-700.

[12] T. P. A. Cao, A. Buchard, X. F. Le Goff, A. Auffrant, C. K. Williams, *Inorg. Chem.* **2012**, *51*, 2157-2169.

[13] A. W. Addison, T. N. Rao, J. Reedijk, J. van Rijn, G. C. Verschoor, *J. Chem. Soc., Dalton Trans.* **1984**, 1349-1356.

[14] R. Duan, C. Hu, X. Li, X. Pang, Z. Sun, X. Chen, X. Wang, *Macromolecules* **2017**, *50*, 9188-9195.

[15] I. M. Marín, A. Audrey, *Eur. J. Inorg. Chem.* **2018**, *2018*, 1634-1644.

[16] J. Adhikary, A. Guha, T. Chattopadhyay, D. Das, *Inorg. Chim. Acta* **2013**, *406*, 1-9.

[17] H. Fujii, Y. Funahashi, *Angew. Chem.-Int. Edit.* **2002**, *41*, 3638-3641.

[18] L. Yang, D. R. Powell, R. P. Houser, *Dalton Trans.* **2007**, 955-964.

[19] A. Buchard, H. Heuclin, A. Auffrant, X. F. Le Goff, P. Le Floch, *Dalton Trans.* **2009**, 1659-1667.

[20] T.-P.-A. Cao, Coordination Chemistry and catalysis with mixed ligands associating iminophosphorane to thiolate or phenolate, Ecole Polytechnique (Palaiseau), **Septembre 2012**.

[21] Y. Tsujimoto, C. Tassel, N. Hayashi, T. Watanabe, H. Kageyama, K. Yoshimura, M. Takano, M. Ceretti, C. Ritter, W. Paulus, *Nature* **2007**, *450*, 1062-1065.

[22] C. Tassel, J. M. Pruneda, N. Hayashi, T. Watanabe, A. Kitada, Y. Tsujimoto, H. Kageyama, K. Yoshimura, M. Takano, M. Nishi, K. Ohoyama, M. Mizumaki, N. Kawamura, J. Íñiguez, E. Canadell, *J. Am. Chem. Soc.* **2009**, *131*, 221-229.

[23] a) X. Wurzenberger, H. Piotrowski, P. Klüfers, *Angew. Chem.-Int. Edit.* **2011**, *50*, 4974-4978; b) S. A. Cantalupo, S. R. Fiedler, M. P. Shores, A. L. Rheingold, L. H. Doerrer, *Angew. Chem.-Int. Edit.* **2012**, *51*, 1000-1005; c) D. Pinkert, S. Demeshko, F. Schax, B. Braun, F. Meyer, C. Limberg, *Angew. Chem.-Int. Edit.* **2013**, *52*, 5155-5158; d) L. Tahsini, S. E. Specht, J. S. Lum, J. J. M. Nelson, A. F. Long, J. A. Golen, A. L. Rheingold, L. H. Doerrer, *Inorg. Chem.* **2013**, *52*, 14050-14063; e) D. Pinkert, M. Keck, S. G. Tabrizi, C. Herwig, F. Beckmann, B. Braun-Cula, M. Kaupp, C. Limberg, *Chem. Commun.* **2017**, *53*, 8081-8084.

[24] a) M. E. Pascualini, N. V. Di Russo, A. E. Thuijs, A. Ozarowski, S. A. Stoian, K. A. Abboud, G. Christou, A. S. Veige, *Chem. Science* **2015**, *6*, 608-612; b) M. E. Pascualini, S. A. Stoian, A. Ozarowski, K. A. Abboud, A. S. Veige, *Inorg. Chem.* **2016**, *55*, 5191-5200.

[25] S.-A. Filimon, D. Petrovic, J. Volbeda, T. Bannenberg, P. G. Jones, C.-G. Freiherr von Richthofen, T. Glaser, M. Tamm, *Eur. J. Inorg. Chem.* **2014**, *2014*, 5997-6012.

[26] B. M. Hakey, J. M. Darmon, Y. Zhang, J. L. Petersen, C. Milsmann, *Inorg. Chem.* **2019**, *58*, 1252-1266.

[27] D. Alhashmialameer, J. Collins, K. Hattenhauer, F. M. Kerton, *Catal. Sci. Technol.* **2016**, *6*, 5364-5373.

[28] H. Zimmer, G. Singh, *J. Org. Chem.* **1963**, *28*, 483-486.

[29] T. Kurahashi, Y. Kobayashi, S. Nagatomo, T. Tosha, T. Kitagawa, H. Fujii, *Inorg. Chem.* **2005**, *44*, 8156-8166.

[30] a) M. Escobar, Z. Jin, B. L. Lucht, *Org. Lett.* **2002**, *4*, 2213-2216; b) A. Matni, L. Boubekeur, N. Mezailles, P. Le Floch, M. Geoffroy, *Chem. Phys. Lett.* **2005**, *411*, 23-27.

[31] A. Böttcher, M. W. Grinstaff, J. A. Labinger, H. B. Gray, *J. Mol. Catal. A-Chem.* **1996**, *113*, 191-200.

[32] K. Matsumoto, H. Egami, T. Oguma, T. Katsuki, *Chem. Commun.* **2012**, *48*, 5823-5825.

[33] R. J. Kern, *J. Inorg. Nucl. Chem.* **1962**, *24*, 1105-1109.

[34] E. M. Schubert, *J. Chem. Educ.* **1992**, *69*, 62.

[35] A. Altomare, M. C. Burla, M. Camalli, G. L. Cascarano, C. Giacovazzo, A. Guagliardi, A. G. G. Moliterni, G. Polidori, R. Spagna, *J. Appl. Crystallogr.* **1999**, *32*, 115-119.

[36] G. M. Sheldrick, SHELXL-97. Universität Göttingen, Göttingen, Germany, **1997**.

[37] L. J. Farrugia, Department of Chemistry, University of Glasgow, **2001**.

[38] G. M. Sheldrick, *Acta Crystallogr. Sect. A* **2008**, *64*, 112-122.

[39] L. Farrugia, *J. Appl. Crystallogr.* **1999**, *32*, 837-838.

WILEY-VCH

Entry for the Table of Contents

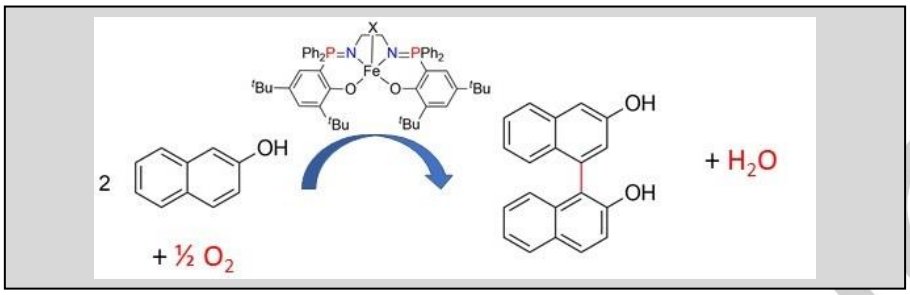

Phosphasalen iron(II) and iron(III) complexes, that differ from their salen analogues by the presence of P=N linkage instead of imine in the ligand backbone, were synthesized and characterized in the solid state and in solution. The Fe^{III} complexes were used to catalyze the oxidative coupling of 1-naphtol using O_2 from air as oxidant.

. ((The Table of Contents text should give readers a short preview of the main theme of the research and results included in the paper to attract their attention into reading the paper in full. The Table of Contents text **should be different from the abstract** and should be no more than 450 characters including spaces.))

Institute and/or researcher Twitter usernames: ((optional))

WILEY-VCH